# Effect of grain geometry on electrical properties of snow at frequencies up to 100 MHz

A. Denoth

Citation: Journal of Applied Physics **53**, 7496 (1982); doi: 10.1063/1.330157
View online: http://dx.doi.org/10.1063/1.330157
View Table of Contents: http://scitation.aip.org/content/aip/journal/jap/53/11?ver=pdfcov
Published by the AIP Publishing



# Effect of grain geometry on electrical properties of snow at frequencies up to 100 MHz

A. Denoth
*Institute of Experimental Physics, University of Innsbruck, A 6020 Austria*

(Received 15 March 1982; accepted for publication 9 July 1982)

The complex dielectric constant of snow samples with different stages of metamorphism and different densities and liquid water contents has been measured in the frequency range of up to 100 MHz. Both the static dielectric constant and the loss factor at frequencies between 1 and 100 MHz depend strongly on the snow texture. The shape of the snow grains or clusters has been found to be an important texture parameter; it is particularly suited for snow classification. A significant influence of the size of the grains on the electrical properties has not been observed. Under the condition of a low ionic conductivity, shape factors to classify snow samples can be derived from the static permittivity. Compared to the determination of shape factors from thin snow sections, the dielectric method is most suitable for application to wet snow.

PACS numbers: 77.20. + y, 61.90. + d, 77.30. + d 92.40.Rm

## I. INTRODUCTION

Commonly used, simple parameters such as mean grain size, porosity, or mean pore diameter are not sufficient to describe the correlation between the texture of snow and its physical properties. Bader[1] showed the importance of the liquid permeability as an index property. But as the relative hydraulic permeability depends on liquid saturation and grain size as well as on the grain shapes and orientation,[2,3] it is only of limited usefulness for snow characterization.

Remote sensing of snow cover characteristics in the microwave region is a valuable data source for modeling the seasonal snowmelt runoff. The microwave response of a snow cover depends distinctly on surface conditions, snow depth, grain size, and grain shape[4]; the scattering coefficient was found to be sensitive to changes in water equivalent and liquid water saturation.[5,6]

Texture parameters like mean grain diameter, grain size distribution, porosity, and especially grain shapes are of particular importance. These parameters and liquid water content control most of the interesting electrical and optical properties of snow. Texture parameters needed to identify the structure may be derived from an analysis of sieve fractions[7] or from thin sections of snow samples using pattern recognition techniques[8]; however, particle shape is more difficult to specify quantitatively.[9] Furthermore, these techniques have not yet been applied to wet snow. Measurements of the influence of snow grain size and grain shape on the static dielectric constant and on the loss factor in the MHz regime are presented here. A method to determine snow grain shapes from the static permittivity is presented. This method is particularly suited for application to wet snow.

## II. SNOW CHARACTERIZATION

In order to account for the influence of the different texture properties on the complex dielectric constant, the snow samples were classified according to grain size, grain shape, and porosity. Snow porosity was calculated from the density $\rho$ and the liquid water content $W$: $\phi = 1 - (\rho - \rho_w W)/\rho_i$. The liquid content was measured by a freezing calorimeter with an absolute accuracy of $\pm 0.5\%$ by volume.

Assuming that the snow grains can be described by ellipsoids of revolution, the shape is characterized by the ratio of the two principal axes $a_1$ and $a_2$ of the spheroid: $m = a_1/a_2$. The mean grain size and axial ratio $m$ were derived from an analysis of photographs of the surface of the snow samples. On the assumption that the snow grains are distributed and orientated randomly, the mean axial ratio $m$ can be calculated from the average axial ratio $\bar{m}$ derived from the projections of the grains in the photograph. A straightforward analysis (see appendix) of the apparent ratio $\bar{m}$ yields:

$$\bar{m} = \frac{2}{\pi}\int_0^{\pi/2} (m^4 + \tan^2\theta)^{1/2} \times (m^2 + \tan^2\theta)^{-1/2} \sin[\theta + atn(m^2/\tan\theta)]\, d\theta. \quad (1)$$

The axial ratio determines the depolarization field inside the snow grains; therefore, most of the electromagnetic properties particularly in the very low ($f < 1$ kHz) frequency regime are controlled not only by the porosity and the liquid water content but also by the shape of the ice grains. The corresponding depolarization factors $g_k$, which are also referred to as shape factors, are correlated to the axial ratio $m$ by[10]:

$$g_1 = g_2 = (1 - g_3)/2,$$
$$g_3 = (1 - m^2)^{-1}[1 - m(1 - m^2)^{-1/2}\cos^{-1}m]. \quad (2)$$

These shape factors are important parameters for the interpretation and calculation of the dielectric constant of a heterogeneous system like snow [cf. Eq. (5)]. Calculations of the axial ratio $m$ for various values of $\bar{m}$ according to Eq. (1) are shown in Fig. 1 as a broken line; calculations of the depolarization factor $g_l$ according to Eq. (2) are shown as a solid line.

To account for the influence of snow texture on the electromagnetic behavior, 53 samples of Alpine-type snow

 0021-8979/82/117496-06$02.40  

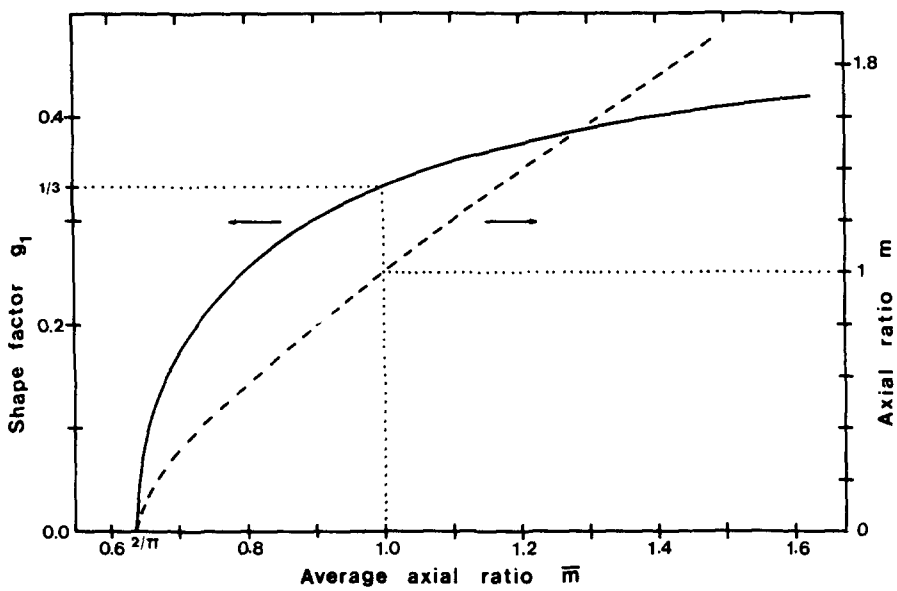


FIG. 1. Calculation of the axial ratio $m$ (broken line) and of the shape factor $g_1$ (solid line) from the photographically determined average axial ratio $\bar{m}$.

have been grouped into three types according to the axial ratio $m$ or the shape factor $g_1$ of the ice grains. Each snow sample has been photographed and the corresponding average axial ratio $\bar{m}$ was derived from an analysis of 100–300 individual grains. The mean axial ratio $m$ and the shape factor $g_1$ were calculated according to Eqs. (1) and (2). A compilation of the characteristic texture parameters is given in Table I. Upper limits for the corresponding errors $E(g_1)$ are also given.

Snow type I is characterized by a large spread in the individual grain sizes, by a mean grain size $d_m < 0.5$, and by porosities ranging between 0.64 and 0.87; the axial ratios $m$ are less than 1:9. This corresponds widely to new snow or to snow which has not undergone appreciable metamorphosis. The temperature of the snow samples was between $-8$ and 0 °C; no melt-freeze cycles were observed. The large error $E(g_1)$ in determining axial ratios or shape factors is a consequence of the inherent difficulties in measuring texture parameters for this type of snow. Therefore, the mean shape factor was not derived and the mean grain size is only a rough estimate. Snow type II is characterized by $0.5 < d_m < 1$ mm, by axial ratios between 1:7 and 1:3.5 of the grains or cluster of grains, and by porosities ranging between 0.48 and 0.73. This corresponds approximately to aged, Alpine snow, some days to weeks old which has undergone melt-freeze cycles. The temperature of the snow samples was 0 °C, the liquid water content was between 0.5% and 8% by volume.

Snow type III is characterized by rounded grains with axial ratios ranging between 1:3 and 1:1, by grain sizes $d_m > 1$ mm, and by porosities between 0.36 and 0.58. This corresponds to old, coarse grained snow or Alpine firn. The temperature of the snow samples was 0 °C, the liquid water content was between 1.5% and 10% by volume.

## III. THE STATIC PERMITTIVITY

In order to derive the static permittivity with high accuracy, the frequency dependence of the complex dielectric constant $\epsilon^*$ was measured in the range of up to 100 MHz. The limiting relative permittivity $\epsilon_s$ was calculated according to the theory of Cole and Cole, which is most suitable to describe the frequency dependence of the dielectric constant of snow.[11] The Cole–Cole formula reads as follows:

$$\epsilon^* = \epsilon_\infty + (\epsilon_s - \epsilon_\infty)[1 + (i\omega\tau)^{1-\alpha}]^{-1}. \quad (3)$$

Plotting the Cole–Cole circle is only an approximate method for obtaining the limiting permittivities.

A straight line representation of Eq. (3) to evaluate the static permittivity $\epsilon_s$ by a least square fit is derived by rationalizing Eq. (3) and by an elimination of $\epsilon_\infty$; it reads as follows:

TABLE I. Texture parameters for the classification of Alpine snow.

| Snow type | $m$ | $g_1$ | Mean shape factor $g_1$ | $E(g_1)$ | Mean grain size $d_m$, mm | Porosity $\phi$ | General remarks |
|---|---|---|---|---|---|---|---|
| I | $<0.11$ | $<0.07$ | — | 0.80 | $<0.5$ | 0.64–0.87 | new, fine grained snow |
| II | 0.14–0.28 | 0.09–0.16 | 0.127 | 0.24 | 0.5–1 | 0.48–0.73 | aged snow |
| III | 0.35–1 | 0.18–0.33 | 0.218 | 0.17 | $>1$ | 0.36–0.58 | old, coarse grained snow, Alpine firn |

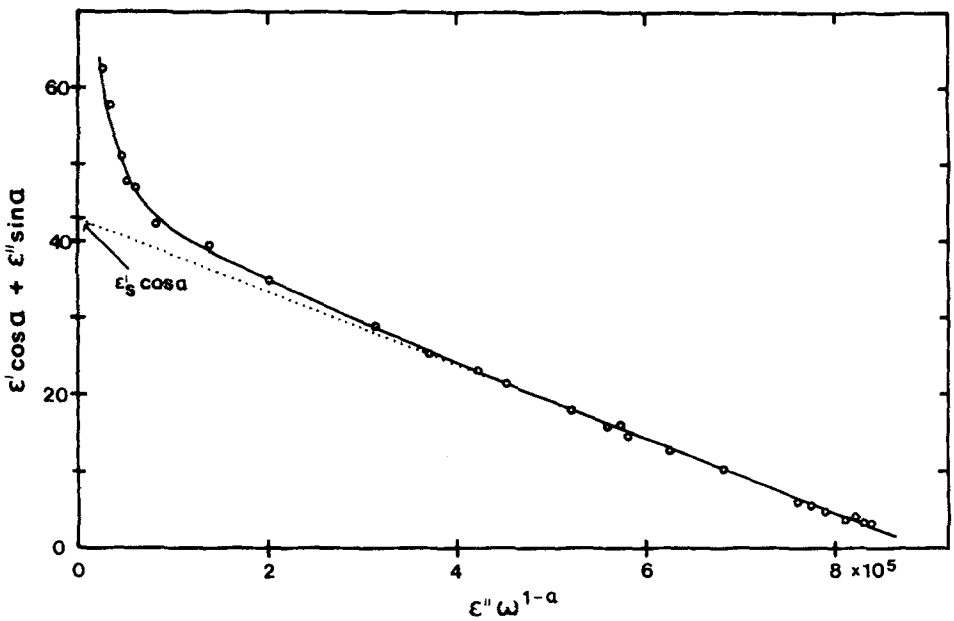


FIG. 2. Determination of the static permittivity $\epsilon_s$ from the measured complex permittivity (solid line with data points) by extrapolation according to the model of Cole and Cole (dotted line).

$$\epsilon' \cos\alpha + \epsilon'' \sin\alpha = \epsilon_s \cos\alpha - \tau^{1-\alpha}\epsilon''\omega^{1-\alpha}. \quad (4)$$

$\epsilon'$ and $\epsilon''$ are the real and imaginary parts of the dielectric constant $\epsilon^*$, $\epsilon_s$ and $\epsilon_\infty$ are the limiting values for $\omega \to 0$ and $\omega \to \infty$, respectively, and $\tau$ represents the characteristic relaxation time. The parameter $\alpha$ determines the width of the distribution function of the relaxation times. A typical evaluation procedure according to Eq. (4) is illustrated in Fig. 2. The characteristic time $\tau$ can be calculated from the slope of the straight line; $\epsilon_s$ follows from the intercept on the axis of the ordinate. The rapid increase of the dielectric constant at low frequencies is due to ionic conductivity.

The dependence of the static permittivity $\epsilon_s$ on porosity $\phi$ for the three different types of snow defined in Table I is shown in Fig. 3. The lines in the figures represent borderline cases of the static relative permittivity for dry snow (solid line) and for wet snow with a 10% liquid content (broken line). Water contents exceeding 10% by volume are not normally found in a natural snow cover. The calculations were made according to the theory of Polder and van Santen.[12]

This theory is of particular importance for modeling the limiting relative permittivities $\epsilon_s$ and $\epsilon_\infty$ of snow as it can account for both the snow texture by means of the shape factors $g_{k,i}$ of the ice grains, and for the structure and distribution of liquid inclusions by means of the shape factors $g_{k,l}$.[13,14] The formula of Polder and van Santen in an adapted form to calculate the static permittivity of snow reads as follows:

$$\epsilon_s\left\{1 - \frac{\epsilon_i - 1}{3}(1-\phi)\sum_k [\epsilon_s + (\epsilon_i - \epsilon_s)g_{k,i}]^{-1}\right\} - 1$$
$$= \frac{\epsilon_w - 1}{3}\epsilon_s W \sum_k [\epsilon_s + (\epsilon_w - \epsilon_s)g_{k,l}]^{-1}, \quad (5)$$

whereby $\epsilon_i$ and $\epsilon_w$ are the static permittivities of ice and water, respectively, $\phi$ means the porosity, and $W$ the liquid water content.

A detailed analysis of the static relative permittivity of snow in different stages of metamorphism shows that $\epsilon_s$ is controlled by the porosity, liquid saturation, and by the

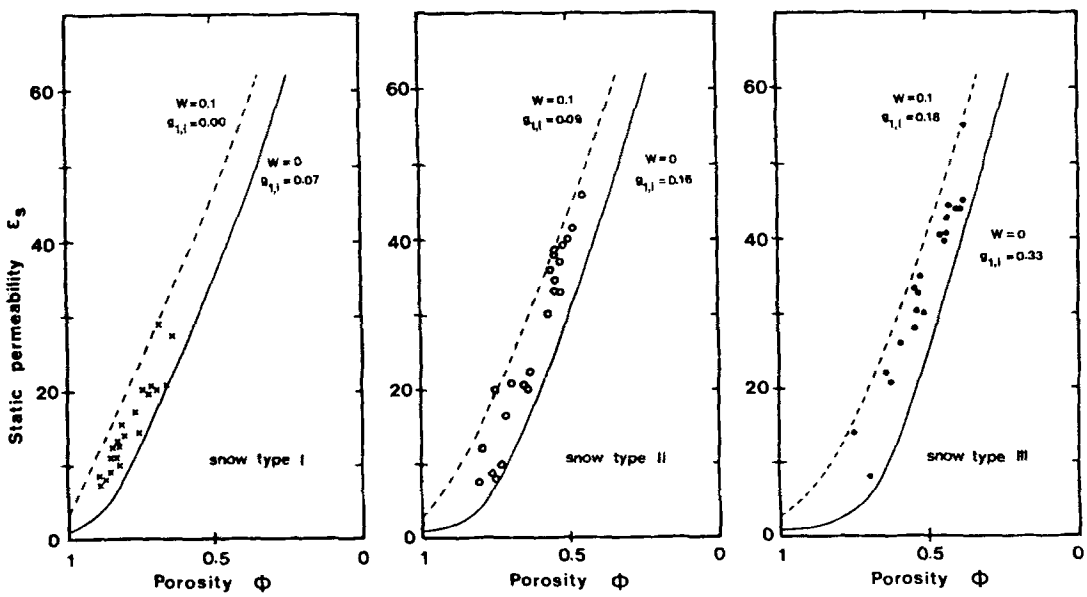


FIG. 3. Experimental results (data points) for the static permittivity $\epsilon_s$ vs porosity $\phi$. Theoretical curves are given for borderline cases: dry snow, solid line, and wet snow ($W = 0.1$), dashed line.

TABLE II. Calculation of the shape factor $g_{1,i}$ of ice grains from $\epsilon_s$.

| Snow type | $\phi$ | $W\%$ | $g_{1,l}$ | $\epsilon_s$ | $E(\epsilon_s)$ | $g_{1,i}$ | $E(g_{1,i})$ | $\epsilon_{\infty,m}$ | $\epsilon_{\infty,c}$ |
|---|---|---|---|---|---|---|---|---|---|
| I | 0.527 | 1.6 | 0.0356 | 33.3 | 0.10 | 0.07 | 0.56 | $2.39 \pm 0.03$ | 2.32 |
| II | 0.760 | 0.0 | 0.0000 | 8.6 | 0.08 | 0.120 | 0.30 | $1.49 \pm 0.05$ | 1.41 |
| III | 0.367 | 8.96 | 0.0720 | 55.2 | 0.03 | 0.210 | 0.20 | $5.20 \pm 0.05$ | 5.20 |

shape of the ice grains or clusters: $\epsilon_s$ reflects texture properties. Because of the comparably high static permittivities of ice,[15] $\epsilon_i = 92$ and water $\epsilon_w = 87.7$ at 0 °C, the effect of liquid distribution may be neglected. A calculation of shape factors according to Eq. (5) for different types of snow is shown in Table II. Data of $g_{k,l}$ to account for the shape of liquid inclusions at different saturations are taken from Denoth.[13] Using the model of Polder and van Santen, the high frequency relative permittivity $\epsilon_{\infty,c}$ is also calculated with the same texture parameters and compared to the measured value $\epsilon_{\infty,m}$.

An error analysis shows that the error $E(g_{1,i})$ is very sensitive to errors in the determination of the static permittivity and in the measurement of snow density. It is comparably easy to measure snow density with the required accuracy; therefore, the accuracy of determining shape factors from the static permittivity is controlled by the error $E(\epsilon_s)$. For the purpose of snow classification with respect to the electromagnetic properties, errors $E(g_{1,i}) < 0.4$ may be acceptable. This means that the errors in determining $\epsilon_s$ should be less than $E(\epsilon_s) < 0.1$: this may be obtained, in general, for snow with a low dc conductivity ($\leqslant 10^{-6}$ mho/m).

## IV. THE LOSS FACTOR

Figure 4 shows the dependence on porosity of the loss factor $\epsilon''$ measured at a frequency of 10 MHz for the different snow types defined in Table I. The solid lines represent a least square fit using Chebyshev polynomials of the third order. Generally, the loss factors increase with decreasing snow porosity. Also, the losses for snow type I, shown in the left plot, are much greater than those for snow type III, shown in the right plot. This behavior may be attributed to the larger specific surface area of the ice grains for snow type I. Experimental data for snow type II are shown in the middle plot. The high frequency loss factor $\epsilon''$, as well as the static permittivity, is highly influenced by snow texture properties. A significant influence of the liquid water content on the loss factor, as it has been measured in the microwave regime,[4,16] has not been observed in the frequency regime of up to 100 MHz. Further investigations and an extended data base are necessary to explain quantitatively the effects of snow texture on the loss factor.

## V. CONCLUSIONS

Based only on the simple texture parameters such as grain size, grain size distribution, and porosity, it is impossible to explain in full detail the electromagnetic characteristics of snow. However, the shape of the snow grains or clusters is an important texture property; it controls both the static dielectric constant and the high frequency losses in the 1–100 MHz regime. A significant influence of the size of the snow grains on the static permittivity and on the high frequency loss factor has not been observed.

Compared to other mixing theories, the model of Polder and van Santen is particularly suited to describe quanti-

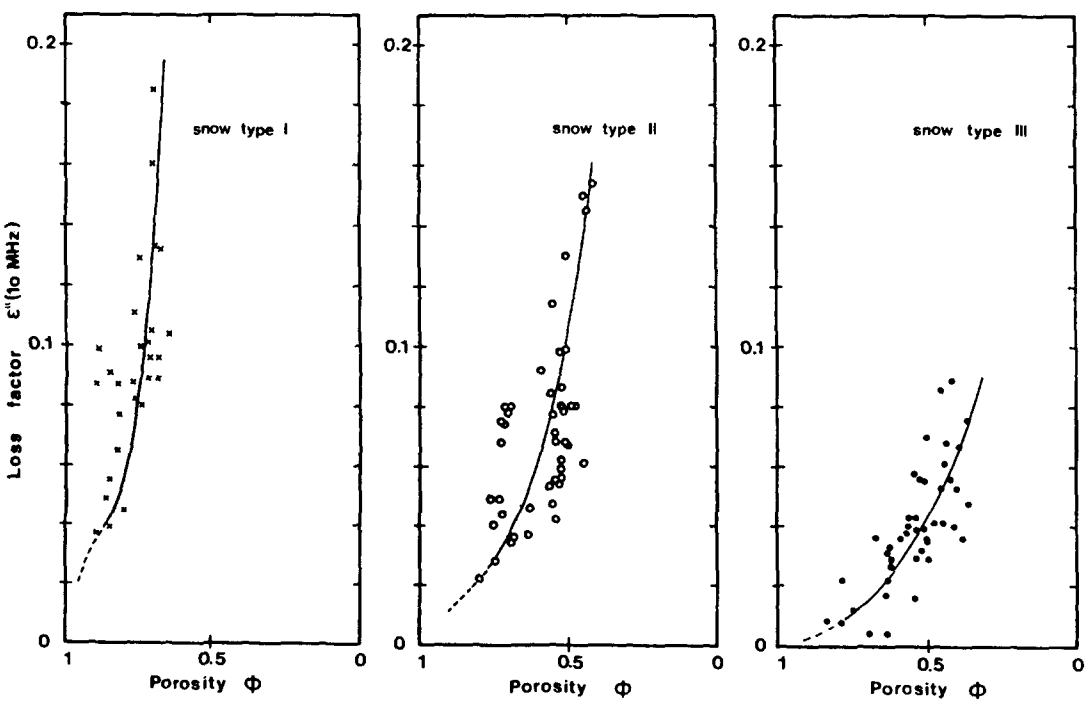


FIG. 4. Experimental results (data points) for the loss factor $\epsilon''$ (10 MHz) vs porosity $\phi$ for snow type I (left plot), snow type II (middle plot), and for snow type III (right plot). The solid lines represent a least square fit.

tatively both the static and high frequency relative permittivity of snow. Furthermore, it accounts for the snow texture and the shape of liquid inclusions by means of the corresponding shape factors.

The shape factor, which is defined by the axial ratio of the snow grains and which controls the electric depolarization field, was found to be a useful parameter for the classification of Alpine snow. For dry snow samples, the shape factor may be obtained from a sieve analysis or from thin sections. These methods are only of limited applicability to wet snow. On the assumption of a low dc conductivity, the calculation of the shape factor from the static dielectric constant may be preferred to the determination from a sieve or photographical analysis; furthermore, this dielectric method is especially applicable to wet snow.


## ACKNOWLEDGMENT

The research reported herein was supported by the Fonds zur Förderung der wissenschaftlichen Forschung, Grant Nos. 3888 and 4525.


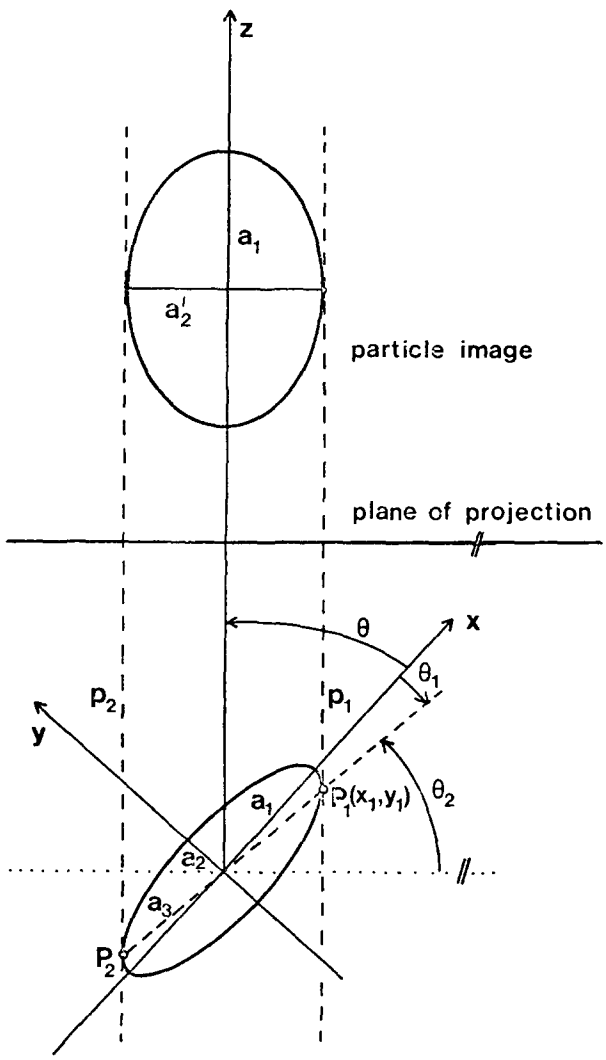


FIG. 1A. Illustration of the geometrical parameters. The half axes of the oblate spheroid are $a_1$ and $a_2$; the half axes in the projection are $a_1$ and $a_2'$.

## APPENDIX

Calculation of the population mean $\bar{m}$ of the axial ratio in the projections of oblate ellipsoids. The parameters used are shown and defined in the Fig. 1A.

$a_2'$, the minimum distance between parallel tangent planes $p_1$ and $p_2$ on the particle, is a function of the orientation $\theta$. It is related to the distance $2a_3$ of the points of contact $P_1$ and $P_2$ by

$$a_2' = a_3 \cos\theta_2,$$

whereby

$$\theta_2 = \frac{\pi}{2} - \theta + \theta_1, \quad \theta_1 = atn\frac{y_1}{x_1},$$

$$\tan\theta = -\left(\frac{a_2}{a_1}\right)^2 \frac{x_1}{y_1},$$

$$\cos\theta_2 = \sin[\theta + atna_2^2/(a_1^2 \tan\theta)].$$

The coordinates of $P_1(x_1, y_1)$ are given by

$$y_1 = a_2^2(a_1^2 \tan^2\theta + a_2^2)^{-1/2},$$

$$x_1 = -a_1^2 \tan\theta(a_1^2 \tan^2\theta + a_2^2)^{-1/2}.$$

The distance $a_3 = (x_1^2 + y_1^2)^{1/2}$ is given by

$$a_3 = (a_2^4 + a_1^4 \tan^2\theta)^{1/2}/(a_2^2 + a_1^2 \tan^2\theta).^{1/2}$$

The axial ratio of the ellipsoid is defined as $a_2/a_1$, the axial ratio in the projection is $a_2'/a_1$. Under the condition that all particles are the same shape ($m = a_2/a_1$ is constant), the population mean[17] $\bar{m}$ of $a_2'/\alpha_1$ (which is a function of orientation $\theta$) is given by

$$\bar{m} = \frac{1}{2\pi}\int_0^{2\pi}\int_\theta \frac{a_2'}{a_1} f(\theta)\,d\theta\,d\varphi.$$

$f(\theta)$ means the probability density function of orientation. Assuming a constant probability function $f(\theta)$, which corresponds to a uniform distribution of orientation, the expectation value $\bar{m}$ is given by

$$\bar{m} = \frac{2}{\pi}\int_0^{\pi/2}\left(\frac{m^4 + \tan^2\theta}{m^2 + \tan^2\theta}\right)^{1/2} \sin\left(\theta + atn\frac{m^2}{\tan\theta}\right)d\theta,$$

whereby, because of symmetry, the limits of integration have been reduced to a single octant.


[1] H. Bader, Cold Regions Science and Engineering, Part II B, edited by F. J. Sanger (U.S. Army Cold Regions Research and Engineering Laboratory, Hanover, New Hampshire, 1962).

[2] A. Denoth, W. Seidenbusch, M. Blumthaler, and P. Kirchlechner, Proc. Modeling of Snow Cover Runoff, Hanover, NH, edited by S. C. Colbeck and M. Ray (1979), pp. 253–256.

[3] K. J. Witt and J. Brauns, Veröffentlichungen Institut f. Bodenmechanik und Felsmechanik, University Fridericana, Karlsruhe, W. Germany, edited by A. Blinde, G. Gudehus, and O. Natau (1981), pp. 81–113.

[4] W. I. Linlor, J. Appl. Phys. **51**, 2811 (1980).

[5] W. H. Stiles, F. T. Ulaby, and A. Rango, Nord. Hydrol. **12**, 143 (1981).

[6] R. Hofer and C. Mätzler, J. Geophys. Res. **85**, C1, 453 (1980).

[7] R. R. Irani and C. F. Callis, *Particle Size: Measurements, Interpretation,*

*and Application* (Wiley, New York, 1963).
[8]C. M. Keeler, Cold Regions Research and Engineering Laboratory, Research Report 271, Hanover, NH (1969).
[9]W. Good, *Pattern Recognition in Practice*, edited by E. S. Gelsema and L. N. Kanal (North Holland Amsterdam, 1980), pp. 161–170.
[10]E. C. Stoner, Philos. Mag. **37**, 7, 263, 803 (1945).
[11]W. Ambach and A. Denoth, Acta Phys. Austriaca **35**, 249 (1972).
[12]D. Polder and J. H. van Santen, Physica **12**, 5, 257 (1946).
[13]A. Denoth, J. Glaciol. **28**, 99 (in press).
[14]S. C. Colbeck, NASA Conf. Publ. CP 2153, 21–39 (1980).
[15]A. D. Watt and E. L. Maxwell, J. Res. Nat. Bur. Stand. Sect. D **64**, 4, 357 (1960).
[16]B. D. Sweeny and S. C. Colbeck, Cold Regions Research and Engineering Laboratory, Research Report 325 (1974).
[17]R. T. DeHoff and F. N. Rhines, *McGraw-Hill Series in Materials Science and Engineering* (McGraw-Hill, New York, 1968).